energies

MDPI

Article

New Time-Frequency Transient Features for Nonintrusive Load Monitoring

Mahfoud Drouaz †, Bruno Colicchio †, Ali Moukadem †, Alain Dieterlen and Djafar Ould-Abdeslam *

IRIMAS, Université de Haute-Alsace, 61 rue Albert Camus, 68093 Mulhouse, France; drouaz_mahfoud@yahoo.fr (M.D.); bruno.colicchio@uha.fr (B.C.); ali.moukadem@uha.fr (A.M.); Alain.dieterlen@uha.fr (A.D.)

* Correspondence: djaffar.ould-abdeslam@uha.fr; Tel.: +33-3-8933-6020

† These authors contributed equally to this work.

Abstract: A crucial step in nonintrusive load monitoring (NILM) is feature extraction, which consists of signal processing techniques to extract features from voltage and current signals. This paper presents a new time-frequency feature based on Stockwell transform. The extracted features aim to describe the shape of the current transient signal by applying an energy measure on the fundamental and the harmonic frequency voices. In order to validate the proposed methodology, classical machine learning tools are applied (k-NN and decision tree classifiers) on two existing datasets (Controlled On/Off Loads Library (COOLL) and Home Equipment Laboratory Dataset (HELD1)). The classification rates achieved are clearly higher than that for other related studies in the literature, with 99.52% and 96.92% classification rates for the COOLL and HELD1 datasets, respectively.

Keywords: nonintrusive load monitoring (NILM); time-frequency transform; Stockwell transform; harmonics; feature extraction

Citation: Drouaz, M.; Colicchio, B.; Moukadem, A.; Dieterlen, A.; Ould-Abdeslam, D. New Time-Frequency Transient Features for Nonintrusive Load Monitoring. *Energies* **2021**, *14*, 1437. https://doi.org/10.3390/en14051437

Academic Editor: Tek Tjing Lie

Received: 10 February 2021
Accepted: 2 March 2021
Published: 5 March 2021

1. Introduction

The massive use of electrical appliances in industrial, residential, and commercial buildings continues to increase. This fact requires a continuous increase in energy production, with the growth in electric energy needs in the last decade reaching 3.4% per year [1,2]. In addition, the diversity of the devices used has increased, especially with the remarkable evolution of technology, most notably in the last few decades. This truth imposes an urgent need to control the energy consumption related to these loads in order to more closely monitor consumption and to act when necessary in the case of anomalies. Some studies estimate the ability to save 20% of the energy consumed if we monitor energy consumption in real time so that we can act in cases of anomalies, most notably in households [3,4]. According to [5], the best way to optimize energy savings is to monitor the consumption per device [1]. This essentially requires load desegregation techniques that can be performed by intrusive or nonintrusive load monitoring methods (ILM or NILM) [6]. Nonintrusive load monitoring (NILM) consists of determining the individual energy consumption of appliances connected to the electrical grid [7]. This can be done by measuring current and voltage signals from one measurement point in order to apply signal processing and machine learning methods to desegregate appliances. The nonintrusive mode is therefore simpler to set up, contrary to the intrusive mode in which measuring equipment must be installed next to each type of load and requires a large number of measuring points. One crucial step in the NILM is feature extraction from voltage and current signals [8]. The objective is to obtain relevant features capable of discriminating between the different types of loads (e.g., linear, nonlinear, and multi-state loads) and at the same time have physical meanings. The NILM features extracted can be divided into two categories: the steady state and transient state. The authors in [8] gave a summary of the proposed NILM features used in the literature. Beyond classical features used for NILM as the step changes in real power

(P) and reactive power (Q) from steady stage [7,9], which quickly showed their limits in the case of nonlinear loads or in the detection of low-power loads, harmonic-based features were massively explored to remedy to these limitations as macroscopic transients combined with harmonic descriptors [10–12]. These also faced certain limitations, particularly that they do not allow a user to discriminate efficiently the nonlinear and multi-state loads [8]. On the other hand, the time-frequency tools proved their utility in studying nonstationary signals, for which statistical characteristics such as a current transient change with time. In the past, time-frequency tools [13–17] were used in the NILM. These studies tried to extract statistical descriptors of time-frequency representation by describing the spectral envelope via short-time Fourier transform (STFT) [18] or by extracting the energy of the wavelet coefficients in each discrete wavelet transform (DWT) level, but none of them focused on the shape of the transient at targeted frequencies, which can be directly related to the physical nature of the load. Other studies were interested in the shape of the current raw signals [19] or the use of VI trajectories in order to more robustly represent the shape of the current and the voltage signals [20]. However, these approaches still suffered from limitations related to the fact that the descriptors are based on the time domain, which can be very sensitive to noise.

Therefore, the aim of this study is to propose qualitative features from the time-frequency domain in order to describe the shape of the electrical transient current signals on a specified frequency range. In other words, we focus on targeted features based on the transient current signals as opposed to traditional approaches consisting of extracting descriptors massively [21] or new blind approaches based on deep learning [22–24]. Moreover, traditional classifiers are used to validate the proposed features since the objective of this paper is not to bring originality to the classification tools but rather to focus on evaluation of the new proposed features. Concerning the available data, for a few years, different datasets have been released, most of them containing signals sampled at low frequencies (1 Hz or less). The low sampling frequency limits the study of descriptors based on harmonics. However, other datasets do exist in the literature with higher sampling frequencies [25–30] to study the transient state. In this paper, in order to validate the proposed approach, we test the proposed features on two datasets: Controlled On/Off Loads Library (COOLL) [26] and Home Equipment Laboratory Dataset (HELD1) [29]. The description of these two datasets are given later. This paper is organized as follow: Section 2 presents the proposed time-frequency features, Section 3 describes the classification tools used in this study in order to evaluate the proposed features. Section 4 is consecrated to the application of the proposed features on two existing datasets: the COOLL [26] and HELD1 datasets [29]. The obtained results are compared with related results in the literature [31] for the COOLL and [29] HELD1 datasets. Finally, Section 5 presents the conclusion and some perspectives related to future work.

2. The Proposed Time-Frequency Features

In this section, we give a brief overview on Stockwell transform before presenting the proposed features based on Shannon energy applied on time-frequency.

2.1. The Stockwell Transform (ST)

The proposed time-frequency features are based on a time-frequency analysis that can be obtained with S-transform [32], defined as a hybrid version between continuous wavelet transform (CWT) and short-time Fourier transform (STFT) [33]. It improves frequency resolution at low frequencies and time resolution at high frequencies in time-frequency representation. For a given signal $x(t) \in L^2(\mathbb{R})$, the S-transform can be defined as follows:

$$ST_x(\tau, f) = \int_{-\infty}^{+\infty} x(t) w(\tau - t, f) e^{-2i\pi f t} \, \mathrm{d}t \tag{1}$$

where $\tau \in \mathbb{R}$ is a time translation and w is a Gaussian window function of time and frequency. It is chosen as follows:

$$w(t,f) = \frac{1}{\sigma(f)\sqrt{2\pi}} e^{-t^2/2\sigma(f)^2} \tag{2}$$

The S-transform is a multi-resolution transform where the dilation σ is a function of frequency and is defined as follows:

$$\sigma(f) = \frac{1}{|f|} \quad f \in \mathbb{R}^* \tag{3}$$

Using this logic for the variation in window width as a function of frequency, we favor temporal resolution for high frequencies since the width of the window is narrower in this case and vice versa for low frequencies.

2.2. The Proposed Time-Frequency Features

We propose a set of features, denoted β_{f_n} that characterize the transient signal. The values β_{f_n} depend on the shape of the transient signal, which is directly related to the physical nature of the load. Therefore, β_{f_n} is calculated on the frequency voices denoted by f_n (fundamental and harmonics frequencies), which can be given as $f_n = \{50,\ 150,\ 250,\ 350,\ \ldots\ n \times 50\ \text{Hz}\}$. The proposed method is summarized in Figure 1.

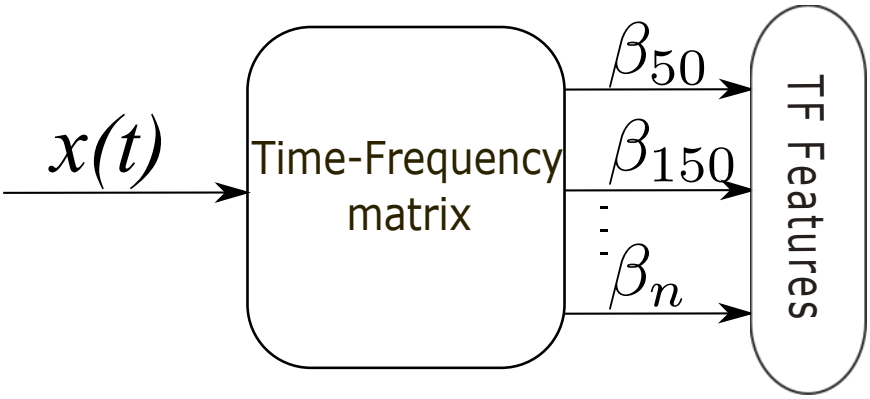

Figure 1. Scheme for extracting β_n features from the time-frequency matrix.

The voice can be seen as the local instantaneous frequency of a signal [32]. By rewriting Equation (1) as a convolution product between the signal $x(t)$ and the Gaussian window $w(t)$ for a particular frequency f_n, the voice calculated on a signal $x(t)$ can be written as follows:

$$ST_x(t,f_n) = \int_{-\infty}^{+\infty} X(\alpha + f_n) e^{2\pi^2\alpha^2/f^2} e^{i2\pi\alpha t}\, \mathrm{d}\alpha \tag{4}$$

where α is related to the frequency translation of the spectrum of signal $x(t)$ and $X(f)$ is the Fourier transform of the signal $x(t)$. This rewriting allows us to take advantage of the Fast Fourier Transform (FFT) algorithm in terms of low computing complexity to generate the time-frequency coefficients. For each localized time and frequency region in the time-frequency plan, the corresponding complex number can be given as follows:

$$ST_x(\tau,f_n) = A(\tau,f_n) e^{i\phi(\tau,f_n)} \tag{5}$$

Before computing the features β_{f_n}, the voice related to f_n needs to be normalized as follows:

$$\overline{ST_x}(t,f_n) = \frac{|ST_x(t,f_n)| - min|ST_x(t,f_n)|}{max(|ST_x(t,f_n)|) - min(|ST_x(t,f_n)|)} \tag{6}$$

The β_{f_n} feature at a specified frequency f_n is then computed by applying the Shannon energy on the module of the corresponding voice:

$$\beta_{f_n} = -\int_{-\infty}^{+\infty} \overline{ST_x}(t,f_n)^2 \log(\overline{ST_x}(t,f_n)^2)\, \mathrm{d}t \tag{7}$$

The logarithmic term in Equation (7) aims to reduce the high and low variation impacts, which usually correspond to noise, and allow us to reduce the intraclass variations. Figure 2 shows the variation in the applied energy measure (Shannon energy) on a linear normalized signal (amplitude varies linearly between 0 and 1). The amplitude of the signal is emphasized in the transformed signal between amplitudes 0.3 and 0.8 and is attenuated elsewhere.

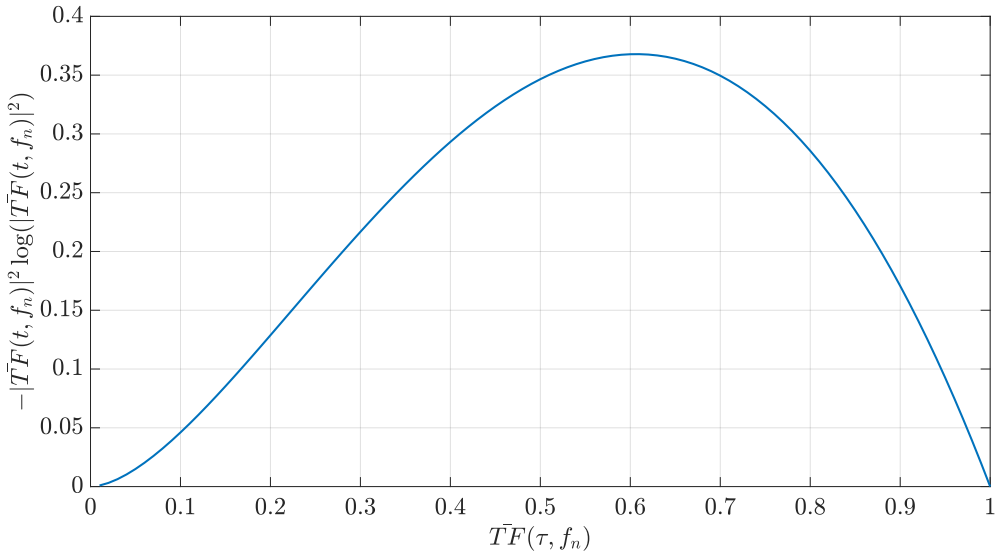

Figure 2. Variation of $-|\overline{ST_x}(t,f_n)|^2\log(|\overline{ST_x}(t,f_n)|^2)$ as a function of the normalized voice $\overline{ST_x}(t,f_n)$.

The advantage of this approach is the rigorous summary of the shape of each envelope of the transient current at the fundamental frequency and its harmonics by a single discriminant feature instead of using an exhaustive feature extraction process.

3. Electrical Load Classification Methodology

To test the performance of the proposed features, we tested them on two distinct databases: COOLL [26] and HELD1 [29]. A brief description of each database and the corresponding results are given in the following sections. The calculated time-frequency features are β_{50}, β_{150} and β_{250}. Taking into account the nature of the loads used in the two bases, it is not necessary to delve further in the harmonic features, but this can be adapted depending on the data and the nature of the used loads. We added to the set of β features the P_{max} feature, which is the maximum value of active power in the transient period. Therefore, the total set of transient features $\mathcal{F}$ used for evaluation in this paper can be given as follows:

$$\mathcal{F} = \{P_{max}, \beta_{50}, \beta_{150}, \beta_{250}\} \quad (8)$$

To evaluate the proposed features, two classical supervised classifiers are used: the k-NN classifier with the euclidean distance and the decision tree with the Gini splitting criterion. For K-NN classifiers, 4 values of K are tested ($K = 3, 5, 7$, and 9). To avoid a random choice from the pair training and validation sets, a cross validation strategy is applied. More precisely, a 10-fold cross validation is used for both classifiers to calculate the classification rate. Therefore, each model is trained using 9 of the folds as training data and the remaining fold is used for the test. Then, a loop is processed to ensure that each fold is used as test data. This validation is repeated 100 times for each feature's combination, and the corresponding results are presented in Section 4.

Applied Analyzing Time-Window

In order to calculate the size of the time window in which we calculate the proposed features, a threshold on the active power is applied. The value of the threshold is set

empirically set to 1.3 W. This value can be adjusted depending on the power of tested appliances. The threshold defines the start and the end instants τ_1 and τ_2 of the time window, which correspond to the beginning and the end of the transient period.

Figure 3 shows the transient current envelope extracted from the fundamental frequency 50 Hz based on a theoretical model presented in [5] with τ_1 and τ_2 instants.

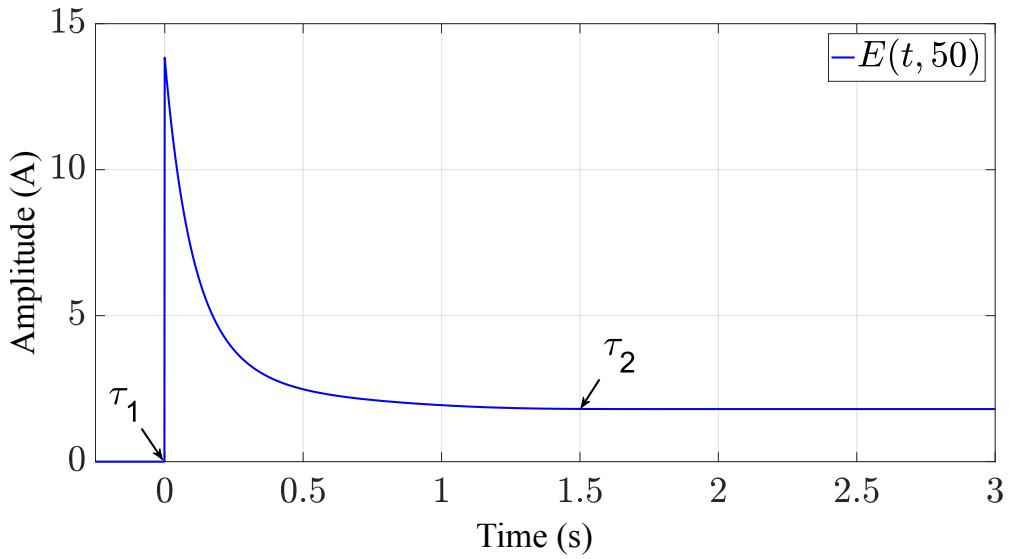

Figure 3. Example of simulated frequency shape of transient current at the fundamental frequency 50 Hz.

Figure 4 shows the result of the theoretical envelopes $E(t, 50)$, $E(t, 150)$, and $E(t, 250)$ calculated from the same transient model [5].

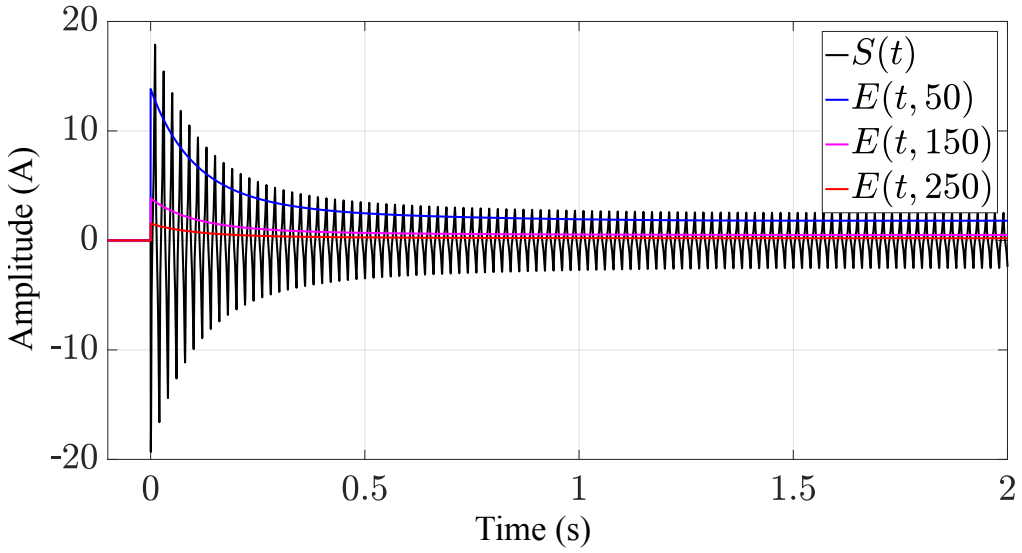

Figure 4. Simulated transient current using model [5] and its frequency shape.

We highlight here that the proposed features in this study do not require any model to estimate them. They are based only on the measured current signal.

4. Results and Discussions

4.1. Datasets Descriptions

4.1.1. COOLL Dataset

Controlled On/Off Loads Library (COOLL) is a high-sampled current and voltage measurement dataset for individual appliance consumption. In total, there are 42 appli-

ances of 12 types measured with 100 kHz sampling frequency. The total measurements in the COOLL dataset is 840 current signals. For each appliance, 20 controlled measurements were made. Each measurement corresponds to a specific action delay ranging from 0 to 19 ms with a step of 1 ms in order to cover the whole time-cycle duration of the 50 Hz main voltage [26]. This base is very useful for testing the robustness of the proposed features against the initial conditions that might affect the waveform of turn-on transients.

4.1.2. HELD1 Dataset

The Home Equipment Laboratory Dataset (HELD1) contains current and voltage signals of turn on and turn off events from 14 different appliances corresponding to 18 different consumers [29]. The sampling rate is 4 kHz, and the total used signatures in this paper is 1365 transient current signals corresponding to 100 on/off events for each device (except for the white refrigerator, where there are only 65 measured events).

4.2. Classification Results

4.2.1. COOLL

The classification rate for the COOLL dataset increases when combining the β features (see Figure 5). P_{max} alone gives a high classification rate (89.88%) already with the K-NN for $K = 9$; see Table 1. It is important to point out that the power-based features are inherently very discriminating (except for load with very close powers). The combination of betas alone without power information show comparable performances (89.88% with the decision tree). This shows the efficiency in describing the transient waveform, which is completely decoupled from power information. The K-NN performance decreases when K increases for the combined β_{50}, β_{150}, and β_{250} features (see Figure 5). A reverse phenomena occurs for individual features (P_{max} or β_{50} alone). The combination of both information (P_{max}, β_{50}) reaches the highest performance: 99.52%, which is higher than the classification rate reached in the literature (98.57%) based on the same dataset in which the authors apply features from a transient model and use the K-NN classifier to classify loads [31]. The confusion matrix for a selected iteration in the K-fold cross validation process obtained on the COOLL dataset shows errors where the Drill load is classified as a Hedge trimmer (see Figure 6). The addition of betas corresponding to higher harmonic shapes does not improve the classification rate; this is strongly linked to the nature of the loads in the dataset.

Table 1. Classification rates of the proposed transient features combined with K-NN and decision tree classifiers applied to Controlled On/Off Loads Library (COOLL) and Home Equipment Laboratory Dataset (HELD1) datasets.

Datasets	**Features**	**Classification Rate (%)**				
		k-NN				**Tree**
		3	**5**	**7**	**9**	
COOLL	P_{max}	88.33	88.93	89.76	**89.88**	88.1
	P_{max}, B_{50}	98.93	98.93	98.69	98.45	**99.52**
	P_{max}, B_{50}, B_{150}	98.45	98.21	97.5	97.02	**99.17**
	P_{max}, B_{50}, B_{150}, B_{250}	98.45	98.21	97.5	97.02	**99.17**
HELD1	P_{max}	81.47	82.27	**82.71**	**82.71**	81.47
	P_{max}, B_{50}	**95.53**	94.8	94.36	94.36	95.38
	P_{max}, B_{50}, B_{150}	95.02	94.87	94.65	94.65	**96.92**
	P_{max}, B_{50}, B_{150}, B_{250}	95.02	94.87	94.65	94.65	**96.92**

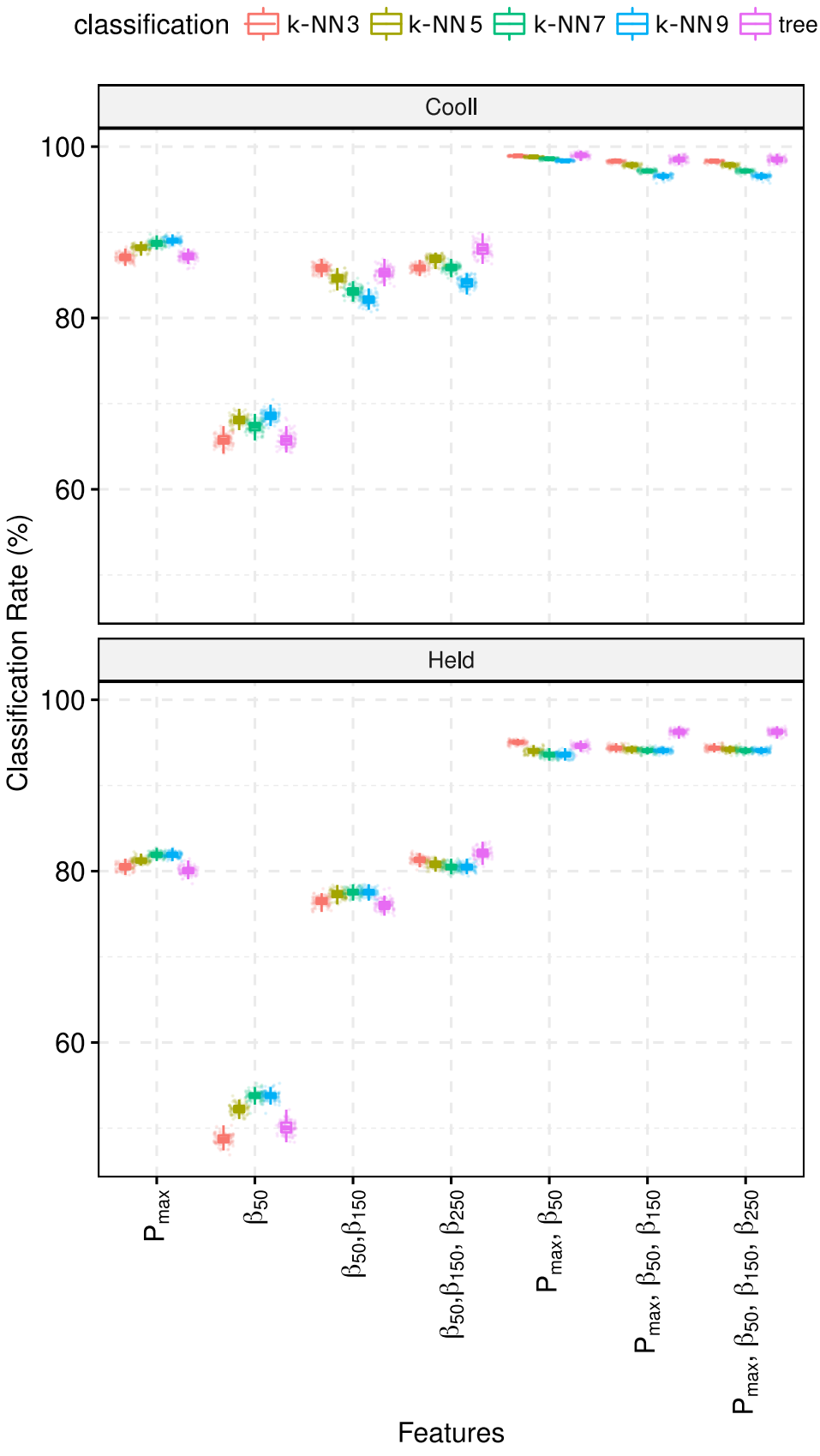

Figure 5. Boxplots of the classification rates for the different tested feature combinations and classifiers (100 repeated K-fold cross validation in each case).

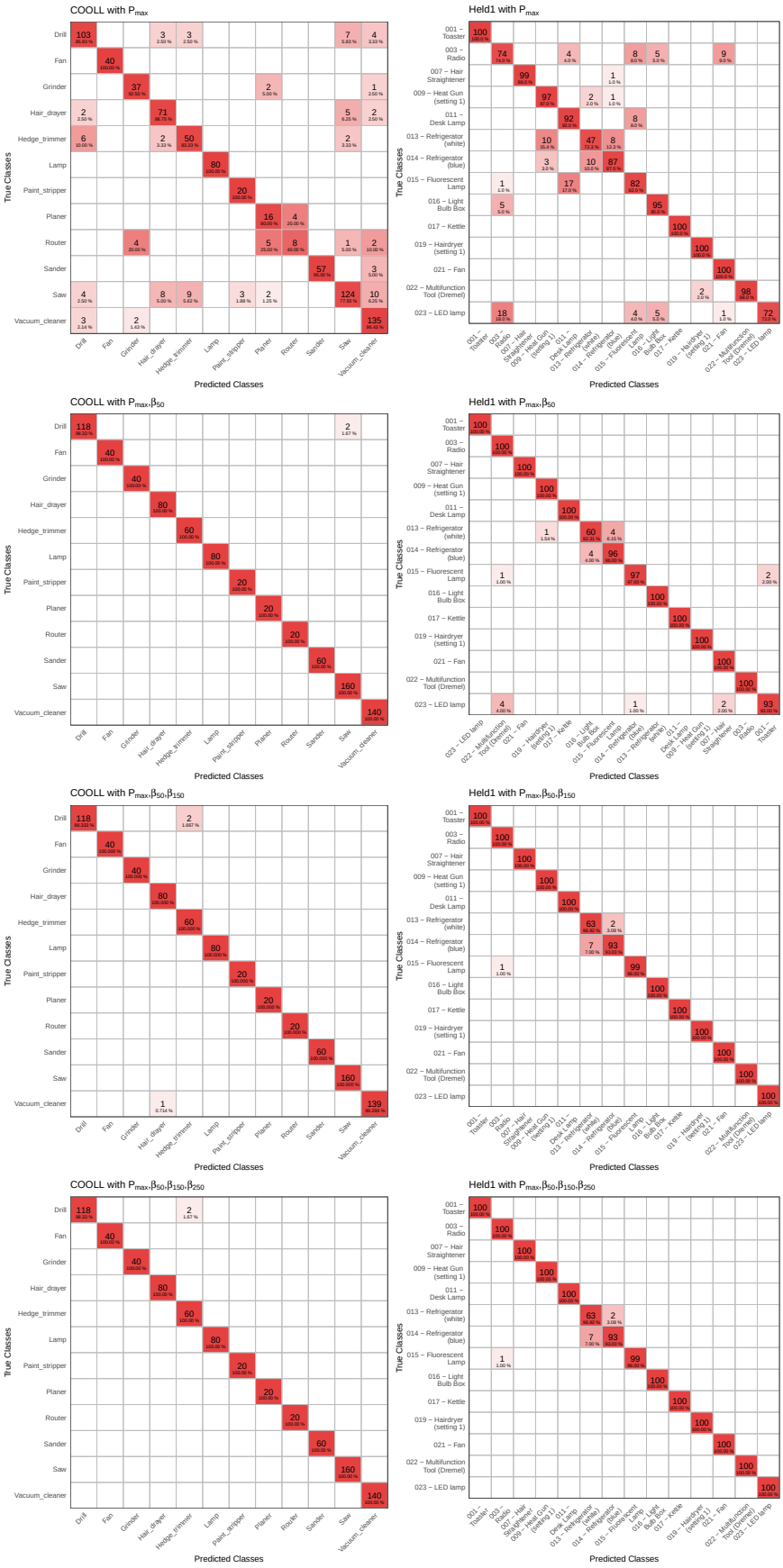

Figure 6. Evolution of the confusion matrices for the highest classification rates obtained on COOLL (**left column**) and HELD1 (**right column**) data for different feature combinations and decision tree classifiers.

4.2.2. HELD1

As in the case of the COOLL dataset, the classification rate of HELD1 shows an increasing trend when aggregating the β features. The highest classification rate 96.92% is reached when combining the P_{max} with β_{50} and β_{150} features and the decision tree classifier. For individual features (P_{max} and β_{50}) and for couple combined features (β_{50} and β_{150}, and P_{max} and β_{50}), the K-NN classifier gives better results than the decision tree. The influence of K for the K-NN is not very significant except for β_{50}, where an improvement in the performance of the classifier can be seen when k is greater than 5 (see Figure 5). For very small values of K, the classifier tends to be overfit by trying to classify isolated points. The same phenomena can be observed for COOLL data and for individual features. The errors obtained on the HELD1 data are due to the fact that the white refrigerator is classified 7 times as a blue refrigerator and that the last one is classified twice as a white refrigerator (see Figure 6).

4.2.3. On the Performance of the Proposed Features

In the case of both bases, the proposed features when tested alone show progressive performance (see Figure 5). As we mentioned before, statistically describing the frequency voices of the transient phases tells us about the physical nature of the load that is completely disconnected from the energy consumption information that is expressed by power. Since the objective of this paper is to explore the advantage of extracting transient phase features, the power information is calculated as the maximum active power (called P_{max}) reached in the transient phase. In both cases (COOLL and HELD1), when adding P_{max} information to the feature's vector, it significantly enhances the classification rate. For COOLL dataset, the improvement is of the order of 10% and 13% for HELD1. The confusion matrices (see Figure 6) clearly show the contribution of the β_n features depending on the nature of the loads. It seems that, for the HELD1 dataset, it is necessary to increase to β_{150}. The classification rate obtained with P_{max}, β_{50} is 95.38%, while the results when adding β_{150} $(P_{max}, \beta_{50}, \beta_{150})$ is 96.92%, which is the higher classification rate for this dataset. In contrast, for the COOLL datset, it is already enough at β_{50}, with the addition of β_{150} and β_{250} not improving the results; on the contrary, it deteriorates them slightly from 99.52% for P_{max}, β_{50} to 99.17% for $P_{max}, \beta_{50}, \beta_{150}$ and $P_{max}, \beta_{50}, \beta_{150}, \beta_{250}$. Adding the β_{250} feature does not improve the performance for COOLL. This means that the information provided by the higher β is too noisy and scattered, which may be due essentially to the nature of the loads that do not have high enough harmonics.

5. Conclusions and Perspectives

This paper presented new transient features based on the time-frequency domain. The objective of the proposed features ws to characterize the turn-on electrical load transients by describing the shape of the frequency harmonic voices. The Stockwell transform was applied in this study to generate the frequency voices. Indeed, other transforms could be used and compared, but the purpose of this paper was to validate the relevance of the proposed approach independent of the used time-frequency transform. By combining the proposed features with P_{max}, which is the maximum active power in the window applied on the transient phase, very high classification rates can be achieved. To validate the proposed approach, the called $\mathcal{F}$ feature set was applied on two public datasets, COOLL and HELD1, with 99.52% and 96.92% reached for the classification rates, respectively. It turns out that, for COOLL data, only the first two features (P_{max} and β_{50}) are sufficient to reach high performance; for HELD1 data, the feature β_{150} must be added to these last features to significantly enhance the classification rate. The β features and their number depend on the nature of the data and the contribution of the harmonics in their loads. Therefore, the proposed number of harmonics features can be adapted according to the data. The obtained results outperform the existing studies in the literature based on the same data [29,31]. It is important to highlight that the presented methodology does not requires a model to estimate the transient parameter, as in [31], which can be changed depending

of the nature of the electrical loads. The tested data are constituted by controlled turn-on loads for both datasets. As future work, more datasets will be tested and the proposed features will be implemented in an embedded system in order to test the classification accuracy in real time.

Author Contributions: Conceptualization, M.D., A.M. and A.D.; formal analysis, M.D., B.C. and A.M.; funding acquisition, D.O.-A.; methodology, M.D., B.C. and A.M.; software, M.D.; supervision, A.D. and D.O.-A.; visualization, M.D. and B.C.; writing—original draft, M.D.; writing—review and editing, B.C. and A.M. All authors have read and agreed to the published version of the manuscript.

Funding: This research received no external funding.

Institutional Review Board Statement: Not applicable.

Informed Consent Statement: Not applicable.

Data Availability Statement: Link to COOLL dataset: https://coolldataset.github.io/ (accessed on 4 March 2021).

Conflicts of Interest: The authors declare no conflicts of interest.

References

1. Schirmer, P.A.; Mporas, I. Statistical and electrical features evaluation for electrical appliances energy disaggregation. *Sustainability* **2019**, *11*, 3222. [CrossRef]
2. Yu, B.; Tian, Y.; Zhang, J. A dynamic active energy demand management system for evaluating the effect of policy scheme on household energy consumption behavior. *Energy* **2015**, *91*, 491–506. [CrossRef]
3. Lee, D.; Cheng, C.C. Energy savings by energy management systems: A review. *Renew. Sustain. Energy Rev.* **2016**, *56*, 760–777. [CrossRef]
4. Zeifman, M.; Roth, K. Viterbi algorithm with sparse transitions (VAST) for nonintrusive load monitoring. In Proceedings of the 2011 IEEE Symposium on Computational Intelligence Applications In Smart Grid (CIASG), Paris, France, 11–15 April 2011; pp. 1–8.
5. Meziane, M.N.; Ravier, P.; Lamarque, G.; Abed-Meraim, K.; Le Bunetel, J.C.; Raingeaud, Y. Modeling and estimation of transient current signals. In Proceedings of the EUSIPCO, Nice, France, 31 August–4 September 2015; pp. 1960–1964.
6. Aladesanmi, E.; Folly, K. Overview of non-intrusive load monitoring and identification techniques. *IFAC-PapersOnLine* **2015**, *48*, 415–420. [CrossRef]
7. Hart, G.W. Nonintrusive appliance load monitoring. *Proc. IEEE* **1992**, *80*, 1870–1891. [CrossRef]
8. Sadeghianpourhamami, N.; Ruyssinck, J.; Deschrijver, D.; Dhaene, T.; Develder, C. Comprehensive feature selection for appliance classification in NILM. *Energy Build.* **2017**, *151*, 98–106. [CrossRef]
9. Drenker, S.; Kader, A. Nonintrusive monitoring of electric loads. *IEEE Comput. Appl. Power* **1999**, *12*, 47–51. [CrossRef]
10. Norford, L.K.; Leeb, S.B. Non-intrusive electrical load monitoring in commercial buildings based on steady-state and transient load-detection algorithms. *Energy Build.* **1996**, *24*, 51–64. [CrossRef]
11. Srinivasan, D.; Ng, W.; Liew, A. Neural-network-based signature recognition for harmonic source identification. *IEEE Trans. Power Deliv.* **2005**, *21*, 398–405. [CrossRef]
12. Dong, M.; Meira, P.C.; Xu, W.; Chung, C. Non-intrusive signature extraction for major residential loads. *IEEE Trans. Smart Grid* **2013**, *4*, 1421–1430. [CrossRef]
13. Lin, Y.H.; Tsai, M.S. Development of an improved time–frequency analysis-based nonintrusive load monitor for load demand identification. *IEEE Trans. Instrum. Meas.* **2014**, *63*, 1470–1483. [CrossRef]
14. Jin, Y.; Tebekaemi, E.; Berges, M.; Soibelman, L. A time-frequency approach for event detection in non-intrusive load monitoring. In Proceedings of the Signal Processing, Sensor Fusion, and Target Recognition XX. International Society for Optics and Photonics, Orlando, FL, USA, 25–27 April 2011.
15. Li, G.; Bo, Y.; ZHU, Z.c. Load Identification of Non-intrusive Load-monitoring System Based on Time-frequency Analysis and PSO-SVM. *DEStech Trans. Eng. Technol. Res.* **2017**. [CrossRef]
16. Su, Y.C.; Lian, K.L.; Chang, H.H. Feature selection of non-intrusive load monitoring system using STFT and wavelet transform. In Proceedings of the 2011 IEEE 8th International Conference on e-Business Engineering (ICEBE), Beijing, China, 19–21 October 2011; pp. 293–298.
17. Duarte, C.; Delmar, P.; Goossen, K.W.; Barner, K.; Gomez-Luna, E. Non-intrusive load monitoring based on switching voltage transients and wavelet transforms. In Proceedings of the Future of Instrumentation International Workshop (FIIW), Gatlinburg, TN, USA, 8–9 October 2012; pp. 1–4.
18. Lee, K.D.; Leeb, S.B.; Norford, L.K.; Armstrong, P.R.; Holloway, J.; Shaw, S.R. Estimation of variable-speed-drive power consumption from harmonic content. *IEEE Trans. Energy Convers.* **2005**, *20*, 566–574. [CrossRef]

19. Suzuki, K.; Inagaki, S.; Suzuki, T.; Nakamura, H.; Ito, K. Nonintrusive appliance load monitoring based on integer programming. In Proceedings of the 2008 SICE Annual Conference, Tokyo, Japan, 20–22 August 2008; pp. 2742–2747.
20. Lam, H.Y.; Fung, G.; Lee, W. A novel method to construct taxonomy electrical appliances based on load signaturesof. *IEEE Trans. Consum. Electron.* **2007**, *53*, 653–660. [CrossRef]
21. Cannas, B.; Carcangiu, S.; Carta, D.; Fanni, A.; Muscas, C. Selection of Features Based on Electric Power Quantities for Non-Intrusive Load Monitoring. *Appl. Sci.* **2021**, *11*, 533. [CrossRef]
22. Houidi, S.; Fourer, D.; Auger, F. On the Use of Concentrated Time–Frequency Representations as Input to a Deep Convolutional Neural Network: Application to Non Intrusive Load Monitoring. *Entropy* **2020**, *22*, 911. [CrossRef] [PubMed]
23. Faustine, A.; Pereira, L.; Bousbiat, H.; Kulkarni, S. UNet-NILM: A Deep Neural Network for Multi-tasks Appliances State Detection and Power Estimation in NILM. In Proceedings of the 5th International Workshop on Non-Intrusive Load Monitoring, Austin, TX, USA, 18 November 2020; pp. 84–88.
24. Ahmed, S.; Bons, M. Edge computed NILM: A phone-based implementation using MobileNet compressed by Tensorflow Lite. In Proceedings of the 5th International Workshop on Non-Intrusive Load Monitoring, Austin, TX, USA, 18 November 2020; pp. 44–48.
25. Kolter, J.Z.; Johnson, M.J. REDD: A public data set for energy disaggregation research. In Proceedings of the Workshop on Data Mining Applications in Sustainability (SIGKDD), San Diego, CA, USA, 21–24 August 2011; pp. 59–62.
26. Picon, T.; Nait Meziane, M.; Ravier, P.; Lamarque, G.; Novello, C.; Le Bunetel, J.C.; Raingeaud, Y. COOLL: Controlled On/Off Loads Library, a Public Dataset of High-Sampled Electrical Signals for Appliance Identification. *arXiv* **2016**, arXiv:1611.05803.
27. Anderson, K.; Ocneanu, A.; Benitez, D.; Carlson, D.; Rowe, A.; Berges, M. BLUED: A Fully Labeled Public Dataset for Event-Based Non-Intrusive Load Monitoring Research. In Proceedings of the 2nd KDD Workshop on Data Mining Applications in Sustainability (SustKDD), Beijing, China, 12–16 August 2012.
28. Gao, J.; Giri, S.; Kara, E.C.; Bergés, M. PLAID: A public dataset of high-resoultion electrical appliance measurements for load identification research: Demo abstract. In Proceedings of the 1st ACM Conference on Embedded Systems for Energy-Efficient Buildings, Memphis, TN, USA, 4–6 November 2014; pp. 198–199.
29. Held, P.; Mauch, S.; Saleh, A.; Benyoucef, D.; Abdeslam, D.O. HELD1: Home Equipment Laboratory Dataset for Non-Intrusive Load Monitoring. In Proceedings of the SIGNAL 2018: The Third International Conference on Advances in Signal, Image and Video Processing, Nice, France, 20–24 May 2018.
30. Renaux, D.P.B.; Pottker, F.; Ancelmo, H.C.; Lazzaretti, A.E.; Lima, C.R.E.; Linhares, R.R.; Oroski, E.; Nolasco, L.D.S.; Lima, L.T.; Mulinari, B.M.; et al. A Dataset for Non-Intrusive Load Monitoring: Design and Implementation. *Energies* **2020**, *13*, 5371. [CrossRef]
31. Meziane, M.N.; Hacine-Gharbi, A.; Ravier, P.; Lamarque, G.; Le Bunetel, J.C.; Raingeaud, Y. Electrical Appliances Identification and Clustering using Novel Turn-on Transient Features. In Proceedings of the ICPRAM, Porto, Portugal, 24–26 February 2017; pp. 647–654.
32. Stockwell, R.G.; Mansinha, L.; Lowe, R. Localization of the complex spectrum: The S transform. *IEEE Trans. Signal Process.* **1996**, *44*, 998–1001. [CrossRef]
33. Battisti, U.; Riba, L. Window-dependent bases for efficient representations of the Stockwell transform. *Appl. Comput. Harmon. Anal.* **2016**, *40*, 292–320. [CrossRef]